ISSN 1027-5495. Functional Materials, 33, No.3 (2026), p. 435-443
doi:http://dx.doi.org/10.15407/fm33.03.435 © 2026 — SSI "Institute for Single Crystals"
This is an open access article under the CC BY-NC-ND license (http://creativecommons.org/licenses/by-nc-nd/4.0/).

Quercetin oxidation catalyzed by CeO_{2-x} and $GdYVO_4:Eu^{3+}$ nanoparticles at physiological pH values

N. Kavok, G. Dudetskaya, V. Seminko*, P. Maksimchuk, V. Klochkov, S. Yefimova

Institute for Scintillation Materials, National Academy of Sciences of Ukraine, 61072, 60 Nauky Ave., Kharkiv, Ukraine
* Corresponding author E-mail: seminko@ukr.net

Received April 4, 2025, approved June 25, 2026

Quercetin (3,3′,4′,5,7-pentahydroxyflavone) is a flavonoid well known for its redox activity, which type (antioxidant or prooxidant) strongly depends on its concentration, pH, and the redox properties of the surrounding biological environment. At alkaline pH (pH > 8), quercetin undergoes autoxidation to semiquinone and quinone species, accompanied by reactive oxygen species (ROS) generation, thus exhibiting pronounced prooxidant behavior. However, the application of quercetin in ROS-mediated anticancer therapy is limited by the slightly acidic extracellular pH of tumor tissues (~6.5–6.9), under which its autoxidation is inefficient. In this study, we demonstrate a significant enhancement of quercetin oxidation in the presence of CeO_{2-x} and $GdYVO_4:Eu^{3+}$ nanoparticles under near-physiological pH conditions (6.7–7.8). Kinetic analysis shows that the experimental data for CeO_{2-x} nanoparticles can be well described by the Michaelis–Menten model. In contrast, this model does not adequately describe the behavior of $GdYVO_4:Eu^{3+}$ nanoparticles. The higher activity of CeO_{2-x} nanoparticles surpassing sufficiently the activity of $GdYVO_4:Eu^{3+}$ ones, can be attributed to the more favorable redox potential of the Ce^{3+}/Ce^{4+} couple compared to the V^{4+}/V^{5+} couple.

Keywords: nanoceria, quercetin, peroxidase, oxidase.

Окиснення кверцетину, каталізоване наночастинками CeO_{2-x} та $GdYVO_4:Eu^{3+}$ при фізіологічних значеннях pH. *Наталія Кавок, Галина Дудецька, Владислав Семінько, Павло Максимчук, Володимир Клочков, Світлана Єфімова*

Кверцетин (3,3′,4′,5,7-пентагідроксифлавон) – це флавоноїд, добре відомий своєю окисно-відновною активністю, тип якої (антиоксидантний або прооксидантний) суттєво залежить від його концентрації, pH та окисно-відновних властивостей навколишнього біологічного середовища. При лужному pH (pH > 8) кверцетин піддається автоокисненню до семіхінонових та хінонових форм, що супроводжується утворенням активних форм кисню (АФК), демонструючи таким чином виражену прооксидантну поведінку. Однак застосування кверцетину в АФК-опосередкованій протипухлинній терапії обмежене слабокислим позаклітинним pH пухлинних тканин (~6,2–6,9), за якого його автоокиснення є неефективним. У цьому дослідженні ми демонструємо значне посилення окиснення кверцетину в присутності наночастинок CeO_{2-x} та $GdYVO_4:Eu^{3+}$ при значеннях pH, близьких до фізіологічних (6,7–7,8). Аналіз кінетики окиснення показує, що експериментальні дані для наночастинок CeO_{2-x} добре описуються моделлю Міхаеліса-Ментен. Натомість ця модель не описує поведінку наночастинок $GdYVO_4:Eu^{3+}$. Вища активність наночастинок CeO_{2-x}, яка значно перевищує активність наночастинок $GdYVO_4:Eu^{3+}$, може бути пов'язана з більш сприятливим значенням окисно-відновного потенціалу пари Ce^{3+}/Ce^{4+} порівняно з парою V^{4+}/V^{5+}.

1. Introduction

Quercetin (3, 3´, 4´, 5, 7-pentahydroxyflavone) is a flavonoid found in fruits and vegetables, which is well-known for its antioxidant [1], anti-inflammatory [2], and antihistamine properties [3]. Recent biomedical studies have shown the ability of quercetin to inhibit lipid peroxidation, platelet aggregation and capillary permeability, and to stimulate mitochondrial biogenesis [4]. Besides, the anticancer effect of quercetin has been documented in numerous *in vitro* and *in vivo* studies that involved several cell lines and animal models [5-7]. The potential role of quercetin in anticancer therapy was reported for breast [8], colon [9], lung [10], prostate [11], ovarian [12] and other cancer types.

One of the possible mechanisms of quercetin anti-tumor activity is related to ROS generation accompanying the processes of autoxidation of quercetin molecules [13]. Quercetin autoxidation is a non-enzymatic oxidation of the molecule by oxygen, typically occurring in aqueous alkaline environments. The autooxidation process involves two subsequent electron transfers to quercetin anions to form *o*-semiquinone radical and quinone molecule as oxidation products. *o*-Semiquinone radical can react with molecular oxygen and give rise to a superoxide anion radical ($O_2^{\bullet-}$), and other ROS producing general pro-oxidant effect [14, 15].

Electron transfer from flavonoids to oxygen can be facilitated by transition metal ions (e.g., Cu^{2+}, Fe^{3+}) or specific enzymes, including cytochrome P450, COX-2, peroxidase, tyrosinase, XO, monoamine oxidase (MAO), and polyphenol oxidases (PPO) [16, 17]. The studies of combined action of quercetin with nanoparticles (NPs) of different types include the research on delivery of quercetin to cancer cells using polymeric [18, 19], mesoporous silica [20], pH-responsive ZnO nanoparticles [21], and iron-containing NPs able to enhance the cytotoxicity of quercetin via Fenton reaction [22]. At the same time, these NPs are used either just as carriers for quercetin molecules, or only slightly modify their ROS generating ability.

Recently, a new type of catalysts based on metal oxide NPs able to facilitate the processes of oxidation of various organic molecules (including biomolecules) was discovered. These NPs, often referred to as *nanozymes* can demonstrate the catalytic activity similar to the one observed for different enzymes [23]. Nanoparticles that exhibit peroxidase-like activity, with oxidation of some substrate molecules along with reduction of hydrogen peroxide, are known as peroxidase-like nanozymes [24]. Peroxidase-like activity of oxide nanoparticles at first was observed for ferromagnetic Fe_3O_4 NPs at low pH, which were found to mimic the catalytic sites of natural peroxidases [25]. This discovery bridged the gap between nanotechnology and enzymology, leading to the identification of several other oxide-based nanozymes, such as cerium oxide [26], and vanadium-based nanozymes [27-29]. The role of Ce^{3+}/Ce^{4+} (V^{4+}/V^{5+}) ions, as well as oxygen vacancies (V_o) in redox activity of these NPs was widely discussed [23, 26-29]. The catalytic ability of nanozymes is generally less than that of natural peroxidases like horseradish peroxidase (HRP). At the same time, oxide NPs with enzyme-like activity offer distinct advantages over natural enzymes, including higher stability under extreme pH and temperature conditions, ease of functionalization, and lower production costs. The combination of highly pH-selective peroxidase activity of oxide NPs with common chemotherapeutic drugs (such as doxorubicin) proved its high efficiency in anticancer therapy [30].

The observed ROS generation as a result of quercetin autoxidation can be considered as a possible pathway for cancer treatment, as high ROS concentrations can trigger cancer cell death in the form of apoptosis or necrosis [31]. At the same time, this approach suffers from the fact that autoxidation of quercetin occurs preferably at alkaline pH, while the medium of cancer cells is slightly acidic (pH ~ 6.5-6.9). At this pH value the spontaneous oxidation of quercetin cannot be enough to produce ROS in concentrations sufficient enough to hamper the growth or metabolism of tumor cells. In this study we have shown the enhancement of quercetin autoxidation processes in the presence of CeO_{2-x} and $GdYVO_4:Eu^{3+}$ nanoparticles, which can be observed at near-physiological pH values (6.7 - 7.8). The enhanced autoxidation of quercetin in the presence of these nanoparticles at slightly acidic pH potentially can be used for ROS generation in extracellular media of cancer cells, for which pH is ~ 6.5-6.9.´

2. Materials and Methods

The synthesis of aqueous ceria nanoparticle dispersions followed a chemical precipitation route. Initially, 100 ml of 2 mM $CeCl_3$ and 100 ml of 4 mM hexamethylenetetramine (HMTA) were combined and stirred at room temperature for 3 hours. Following the addi-

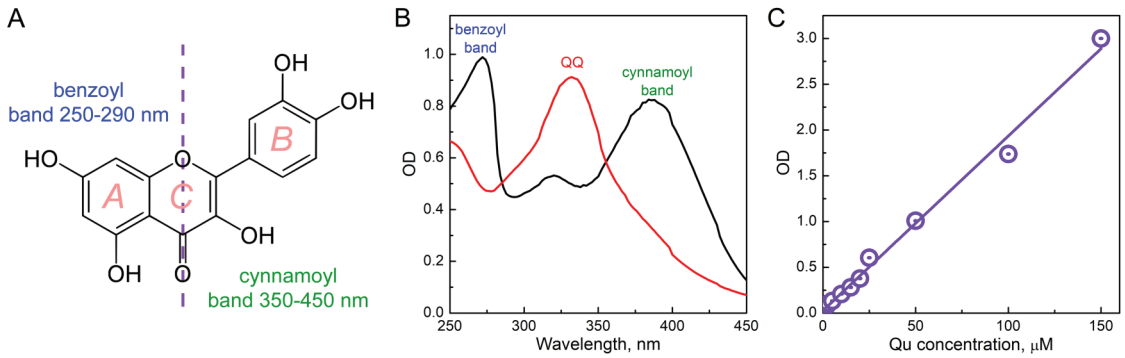

Fig. 1. A) Structure of quercetin molecule; B) Absorption spectra of quercetin molecule before (black) and after oxidation (red); C) Calibration curve relying quercetin (Qu) concentration and optical density at 370-380 nm.

tion of 1.8 ml of 25% NH_4OH and 0.6 ml of 60% H_2O_2, the mixture was refluxed in a round-bottom flask for 5 hours, yielding a transparent solution. The resulting liquid was concentrated to 30 ml via rotary evaporation. To isolate the solid phase, 3 ml of 2 M $CaCl_2$ was added to induce turbidity, followed by centrifugation. The precipitate was separated and the procedure was repeated. After that the distilled water was added and the precipitate was separated by centrifugation. The final precipitate was redispersed in 30 ml of distilled water and an aqueous sodium citrate solution was added at a CeO_2/NaCt molar ratio of 1:1. The final transparent products were filtered through ultrafilters with 100 nm pores. The size of NPs was ~ 2 nm. Full characterization of obtained NPs (including TEM, XRD, DLS, zeta potential, and XPS) can be found in our book [32].

The $GdYVO_4:Eu^{3+}$ aqueous colloidal solutions were synthesized as follows. 10 ml of 0.01 M gadolinium/yttrium chloride solution was combined with 8 ml of 0.01 M sodium citrate. Under vigorous magnetic stirring, 8 mL of Na_3VO_4 (0.01 M, pH 13) was introduced dropwise to the mixture. Stirring continued until a transparent yellowish solution formed. The mixture was thermally treated in 100 °C water bath. Finally, the solutions were cooled and purified via 24-hour dialysis against deionized water using a 12 kDa molecular weight cut-off membrane to eliminate residual ions. The size of NPs was ~ 2 nm. Additional Eu^{3+} doping providing luminescent properties of NPs was achieved by addition of europium chloride solution during synthesis. Full characterization of obtained NPs (including TEM, XRD, DLS, zeta potential, and XPS) can be found in our previous study [33].

The kinetic parameters of the oxidase (OXD)-like and peroxidase (POD)-like activities of the NPs towards quercetin were determined in 10 mM Tris buffer by UV-Vis absorption measurements using Varioskan LUX Multimode Microplate Reader (Thermo Scientific) at pH 6.7 (λ_{ma} = 371 nm), pH 7.4 (λ_{max}= 380 nm), and pH 7.8 (λ_{max} = 387 nm). The concentration of NPs in all experiments was 20 μg/ml. The quercetin concentration ranged from 25 to 75 μmol/l, and the POD-like reaction was initiated by the addition of 1.6 mM of H_2O_2.

Means were calculated from at least three independent experiments. Analysis of statistical significance was performed by ANOVA followed by Bonferroni's post hoc test.

3. Results and discussion

The chemical structure of quercetin molecule is shown in the Fig. 1A. Quercetin molecule consists of two benzene rings (denoted as A and B) connected by a central pyran ring (ring C), and possesses five hydroxyl (-OH) groups at positions 3, 5, 7, 3′, 4′. Optical properties of quercetin are determined by conjugated pi-orbitals of cinnamoyl (ring B and part of ring C), and benzoyl (ring A and part of ring C) systems. Accordingly, absorption spectra of quercetin exhibit two characteristic peaks at 350–390 nm (cinnamoyl system), and around 250–270 nm (benzoyl system) (Fig. 1B) [26].

In the presence of oxygen quercetin molecule undergoes autooxidation accompanied by formation of short-lived quercetin-semiquinone ($Q^{\bullet -}$) radicals and superoxide anions ($O_2^{\bullet -}$): $Q^- + O_2 \rightarrow Q^{\bullet} + O_2^{\bullet -}$. The semiquinone radical doesn't stay in that state for long. It quickly undergoes a second electron transfer either by reacting with another oxygen molecule to form quercetin-quinone (QQ), the oxidized form of quercetin. This process occurs with formation of additional superoxide radicals: $Q^{\bullet -} + O_2 \rightarrow$

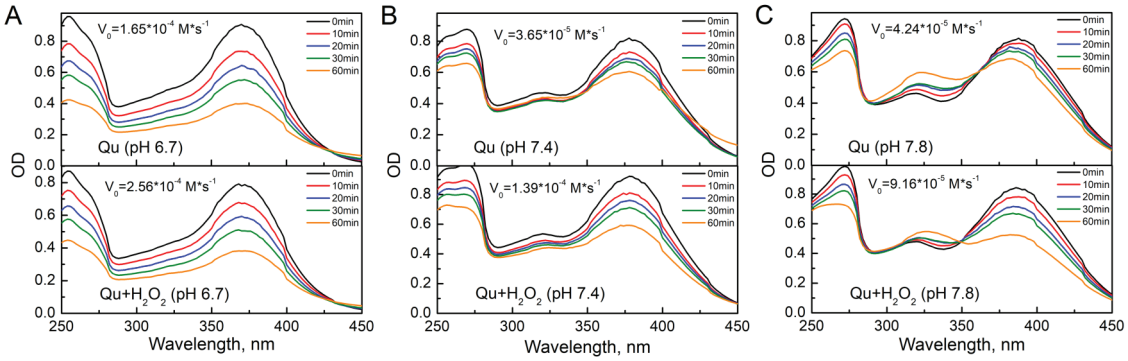

Fig. 2. Time dependences of quercetin absorption spectra during quercetin autooxidation at different pH values (A – pH 6.7, B – pH 7.4, C – pH 7.8) without and in the presence of H_2O_2.

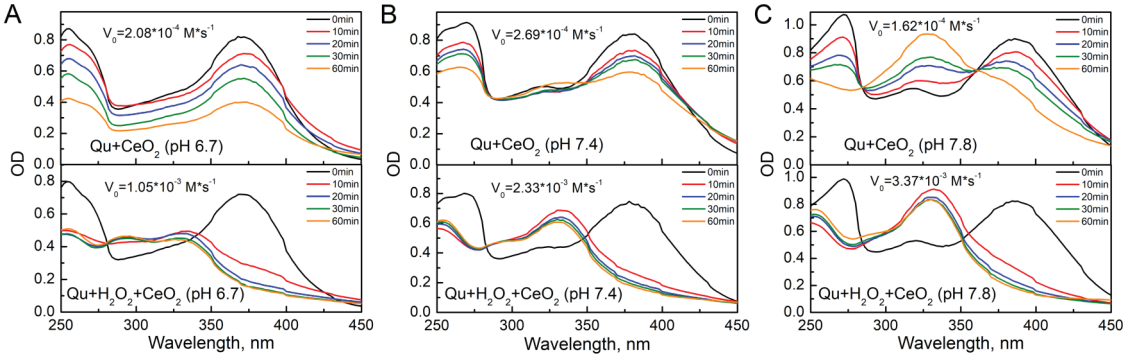

Fig. 3. Effect of CeO_{2-x} NPs on the time dependences of quercetin absorption spectra during quercetin autooxidation at different pH values (A – pH 6.7, B – pH 7.4, C – pH 7.8) without and in the presence of H_2O_2.

QQ + $O_2^{\bullet-}$. The oxidation of quercetin occurs primarily on the cinnamoyl side of the molecule leading to shortening of its pi-conjugated system and blue shift of the cinnamoyl band to 300–310 nm (quercetin-quinone band), with further shift to ~290 nm if oxidation continues [34]. Therefore, the dynamics of 350–390 nm absorption band decrease in the spectra of quercetin molecule undergoing autooxidation can be considered as a reliable measure of the rate of oxidation, as well as the rate of superoxide generation inevitably accompanying this process.

The rate of quercetin autooxidation can be sufficiently increased by both external conditions (pH, temperature) and presence of catalysts. In this study we have determined the effect of CeO_{2-x} and $GdYVO_4$:Eu^{3+} nanoparticles on the rate of quercetin oxidation at different pH values. As an additional oxidant hydrogen peroxide (H_2O_2) as used, which is an omnipresent type of ROS, which concentration is especially high in cancer cells [31]. In order to determine the time dependence of quercetin concentration (and so, the rate of quercetin oxidation) from the absorption spectra, the calibration curve (Fig. 1C) was obtained.

Figure 2 shows the oxidation of quercetin without NPs. Both absorption peaks of quercetin (related to cinnamoyl and benzoyl system) decrease indicating slow oxidation of quercetin to quercetin-quinone. The rates of quercetin oxidation (V_0) determined from the spectra at t = 0-60 min using the calibration curve (Fig. 1C) depend sufficiently on pH value. The increase of quercetin oxidation rates at higher pH values can be attributed to enhanced deprotonation of hydroxyl groups, which increases electron density in the aromatic system and facilitates oxidation to semiquinone and quinone-like structures [34]. Another effect of deprotonation is a bathochromic shift of cinnamoyl band from 370 nm at pH 6.7 to 380 nm at pH 7.4, and to 388 nm at pH 7.8. The rate of quercetin oxidation further increases in the presence of hydrogen peroxide.

Figure 3 shows the effect of CeO_{2-x} nanoparticles on quercetin oxidation. In the absence of hydrogen peroxide, CeO_2 induces only minor effect on the quercetin oxidation rate. When hydrogen peroxide is added, the spectral evolution becomes much more pronounced. Cinnamoyl band rapidly decreases, and a broad absorption band develops at ~320-330 nm

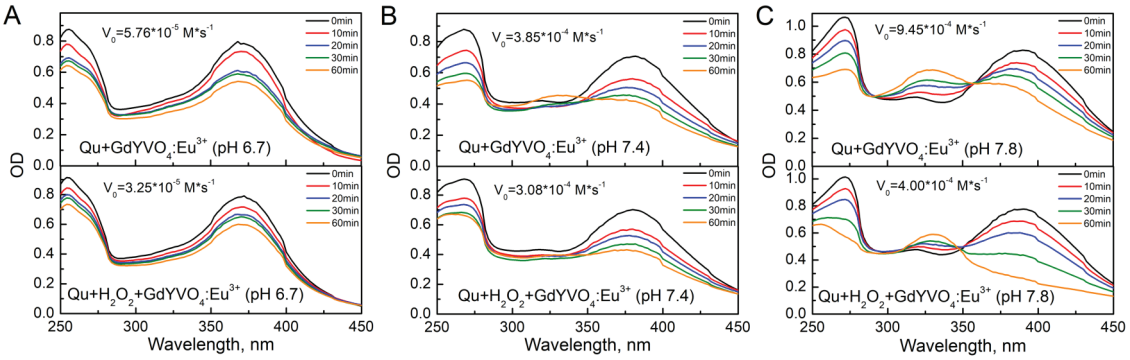

Fig. 4. Effect of $GdYVO_4:Eu^{3+}$ NPs on the time dependences of quercetin absorption spectra during quercetin autooxidation at different pH values (A – pH 6.7, B – pH 7.4, C – pH 7.8) without and in the presence of H_2O_2.

related to fully oxidized quercetin (quercetin-quinone), indicating efficient catalytic oxidation of quercetin. The rates of quercetin oxidation in the presence of CeO_{2-x} nanoparticles increase in 5 to 30 times depending on pH value: from $2.56 \cdot 10^{-4}$ M·s^{-1} to $1.05 \cdot 10^{-3}$ M·s^{-1} at pH 6.7, from $1.39 \cdot 10^{-4}$ M·s^{-1} to $2.33 \cdot 10^{-3}$ M·s^{-1} at pH 7.4, and from $9.16 \cdot 10^{-5}$ M·s^{-1} to $3.37 \cdot 10^{-3}$ M·s^{-1} at pH 7.8. Such a sufficient enhancement of quercetin oxidation in the presence of CeO_{2-x} nanoparticles indicates a role of nanoceria as a catalyst in the process of quercetin degradation. This behavior is consistent with the well-known redox cycling between Ce^{3+} and Ce^{4+} on the nanoparticle surface, which facilitates reactive oxygen species generation at acidic pH [35]. Therefore, the resulting change of the absorption spectra is a result of combination of pH effect on the quercetin autoxidation itself (enhanced deprotonation at high pH) and on the peroxidase-like activity of nanoceria, which increases at pH decrease.

Figure 4 presents the effect of $GdYVO_4:Eu^{3+}$ nanoparticles on the process of quercetin oxidation without and with hydrogen peroxide. Both in the absence and presence of hydrogen peroxide, moderate increase of quercetin oxidation is observed, however, these changes are less pronounced compared to those observed with ceria, suggesting lower intrinsic catalytic activity.

Overall, the results demonstrate that quercetin oxidation is strongly pH-dependent and its rate can be significantly accelerated by hydrogen peroxide and presence of NPs. For the sake of comparison, the initial oxidation rates (V_0) determined from Figs. 2-4 using calibration curve (Fig. 1C) are shown in the Figure 5A for different NPs and pH values. For all combinations of NPs and oxidants the quercetin oxidation rates increases at pH increase from 6.7 to 7.8. This effect is related to quercetin oxidation properties itself as at high pH quercetin has higher tendency to lose protons from one of its more acidic hydroxyl groups (mainly, 4'-OH) that simplifies further oxidation of this molecule [34].

In the presence of CeO_{2-x} NPs and H_2O_2 the rate of quercetin oxidation increases drastically (from 5 to 30 times) depending on pH value. This effect can be related to catalytic (peroxidase-like) activity of CeO_{2-x} NPs, i.e. the ability of these NPs to enhance the processes of oxidation of substrates (in this case, quercetin) by hydrogen peroxide.

For NPs with enzyme-like activity the dependence of the substrate conversion rate on the substrate concentration should follow the Michaelis-Menten kinetics widely used to analyze the activity of biological enzymes [36] and recently successfully applied for nanozymes [37]:

$$V = \frac{V_{max}[S]}{K_m + [S]} \quad (1)$$

In equation (1), V is the rate of oxidation, V_{max} is the maximum oxidation rate observed at saturating substrate (quercetin or oxidant) concentration, [S] is the substrate concentration, and K_m is the Michaelis constant, which is equivalent to the substrate concentration in which the rate of conversion is half of V_{max}. This model predicts saturation effect at high substrate concentration due to limited number of binding sites of enzyme molecule (or on the surface of nanoparticle).

The increase of quercetin concentration led to an increase in the rate of quercetin oxidation for both types of NPs with or without H_2O_2 with saturation effect at quercetin concentration of about 50 μM. The applicability of Michaelis-Menten model was determined using

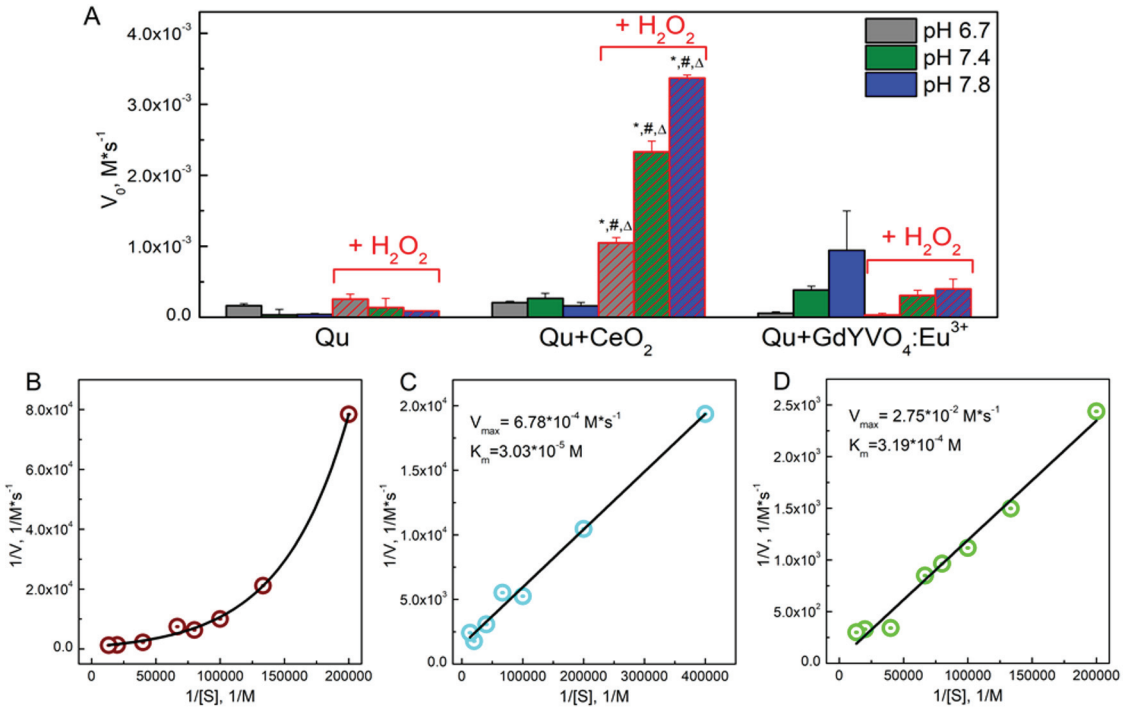

Fig. 5. A) The effect of NPs and pH on the initial rate (V_0) of quercetin autooxidation; B-D) The Lineweaver-Burk plots for quercetin autooxidation rates in the presence of $GdYVO_4:Eu^{3+}$ NPs (B), CeO_{2-x} NPs (C), CeO_{2-x} NPs with H_2O_2 (D). *- $p < 0.0083$ compared to l Qu control ((+) H_2O_2); # - $p < 0.0083$ compared to own Qu + CeO_{2-x} control ((-) H_2O_2); Δ – $p < 0.0083$ compared to Qu + $GdYVO_4:Eu^{3+}$((+)H_2O_2).

Lineweaver-Burk plots, i.e. the linear form of Michaelis-Menten:

$$\frac{1}{V} = \frac{1}{V_{max}} + \frac{K_m}{V_{max}[S]} \qquad (2)$$

The dependences of inverse oxidation rates (1/V) on the inverse quercetin concentrations (1/[S]) for the samples with varied quercetin concentration and fixed concentration of NPs are shown in Fig. 5 (B-D). As can be seen from the Fig. 5 B, the experimental data for $GdYVO_4:Eu^{3+}$ nanoparticles in the Lineweaver-Burk coordinates cannot be fitted by a straight line in the whole range of quercetin concentrations and so, do not follow Michaelis-Menten kinetics. At the same time, the dependences obtained for the samples with CeO_{2-x} nanoparticles both without (Fig. 5C) and with H_2O_2 (Fig. 5D) are well described by eq. (2) confirming the applicability of this model. The oxidase-like (with oxygen as oxidant) and peroxidase-like (with hydrogen peroxide as oxidant) activities of CeO_{2-x} nanoparticles were previously reported for a number of substrates including TMB (3,3',5,5'-tetramethylbenzidine) [38], OPD (*o*-phenylenediamine) [39], and ABTS (2,2'-azino-bis(3-ethylbenzothiazoline-6-sulfonic acid)). At the same time, the maximum efficiency of peroxidase-/oxidase-like activity of CeO_{2-x} nanoparticles for all these substrates were observed at extremely low pH values (pH 3.5 – 5.5), which are sufficiently less than the ones typical for microenvironment of cancer cells (pH 6.5–6.9). Notably, the sufficient effect of CeO_{2-x} nanoparticles on the quercetin autooxidation are observed at pH values close to the ones typical for tumor microenvironment can be perspective for obtaining efficient prooxidant materials.

The comparably low effect on the $GdYVO_4:Eu^{3+}$ nanoparticles on the quercetin autooxidation rate, and inadequacy of Michaelis-Menten model for these nanoparticles require separate discussion. As was shown previously in the number of studies, enzyme-like activities including as antioxidant (catalase-like and superoxide dismutase-like), as well as prooxidant ones (peroxidase-like and oxidase-like) of nanoceria are determined by active sites formed by oxygen vacancies and/or Ce^{3+} ions [40]. In [41] as active sites for CeO_{2-x}-H_2O_2 interaction Ce^{3+} - Vo - Ce^{3+} complexes were proposed, where V_O is oxygen vacancy. The formation of such complexes on the ceria (111) surface is highly energetically favorable, and this fact along with high redox potential of Ce^{3+}/Ce^{4+} at physiological pH determines the ability of nanoceria to take part in various

redox reactions with recovery of initial state afterwards. The previously determined value of redox potential of Ce^{3+}/Ce^{4+} at slightly acidic pH equal to ~ +0.6 V [42] is optimal for catalytic quercetin oxidation as quercetin shows its first oxidation step (catechol - semiquinone) at about +0.2 to +0.4 V, and the second oxidation step (toward QQ formation) at around +0.5 to +0.7 V at neutral or slightly acidic pH. At the same time, although the V^{4+}/V^{5+} redox pair in $GdYVO_4:Eu^{3+}$ nanoparticles is theoretically capable of participating in quercetin oxidation processes, the redox potential of this pair at neutral or slightly acidic pH (~ +0.3 V) [43] is less favorable for quercetin oxidation. This fact along with absence of Michaelis-Menten kinetics for $GdYVO_4:Eu^{3+}$ nanoparticles determine their inefficiency in quercetin oxidation both in direct and catalytic way.

4. Conclusions

CeO_{2-x} and $GdYVO_4:Eu^{3+}$ nanoparticles enhance quercetin oxidation in water solutions under near-physiological pH conditions (6.7–7.8). Kinetic analysis reveals that the catalytic activity of CeO_{2-x} nanoparticles follows the Michaelis–Menten model, indicating pronounced oxidase- and peroxidase-like behavior. In contrast, the oxidation process in the presence of $GdYVO_4:Eu^{3+}$ nanoparticles does not conform to this model, suggesting a different, probably, non-enzymatic mechanism. This effect is attributed to the more favorable redox properties of the Ce^{3+}/Ce^{4+} couple compared to the V^{4+}/V^{5+} couple influencing the efficiency of electron transfer processes. Overall, these findings highlight the potential of cerium oxide NPs to promote quercetin oxidation and ROS generation under physiologically relevant conditions, offering a promising approach for enhancing its prooxidant activity.

Acknowledgements:

This research was supported by National Research Foundation of Ukraine, Grant № 2023.03/0050.

References:

1. D. Xu, M.J. Hu, Y.Q. Wang, Y.L. Cui, Antioxidant activities of quercetin and its complexes for medicinal application, *Molecules* 24 (2019) 1123. https://doi.org/10.3390/molecules24061123
2. R. Kleemann, L. Verschuren, M. Morrison, S. Zadelaar, M.J. van Erk, P.Y. Wielinga, T. Kooistra, Anti-inflammatory, anti-proliferative and anti-atherosclerotic effects of quercetin in human in vitro and in vivo models, *Atherosclerosis* 218 (2011) 44–52. https://doi.org/10.1016/j.atherosclerosis.2011.04.023
3. Y. Li, J. Yao, C. Han, J. Yang, M.T. Chaudhry, S. Wang, Y. Yin, Quercetin, inflammation and immunity, *Nutrients* 8 (2016) 167. https://doi.org/10.3390/nu8030167
4. L. Aguirre, N. Arias, M.T. Macarulla, A. Gracia, M.P. Portillo, Beneficial effects of quercetin on obesity and diabetes, *Open Nutraceuticals J.* 4 (2011) 189–198. 10.2174/1876396001104010189
5. A. Rauf, M. Imran, I.A. Khan, M. ur-Rehman, S.A. Gilani, Z. Mehmood, M.S. Mubarak, Anticancer potential of quercetin: A comprehensive review, *Phytother. Res.* 32 (2018) 2109–2130. https://doi.org/10.1002/ptr.6155
6. A. Massi, O. Bortolini, D. Ragno, T. Bernardi, G. Sacchetti, M. Tacchini, C. De Risi, Research progress in the modification of quercetin leading to anticancer agents, *Molecules* 22 (2017) 1270. https://doi.org/10.3390/molecules22081270
7. Y. Afşin, S. Alkan Akalın, İ. Özdemir, M.C. Tuncer, Ş. Öztürk, Molecular Insights into the Synergistic Anticancer and Oxidative Stress–Modulating Activity of Quercetin and Gemcitabine, *Antioxidants*, *15* (2026) 91. https://doi.org/10.3390/antiox15010091
8. L.T. Nguyen, Y.H. Lee, A.R. Sharma, J.B. Park, S. Jagga, G. Sharma, J.S. Nam, Quercetin induces apoptosis and cell cycle arrest in triple-negative breast cancer cells through modulation of Foxo3a activity, *Korean J. Physiol. Pharmacol.* 21 (2017) 205–213. https://doi.org/10.4196/kjpp.2017.21.2.205
9. J.Y. Kee, Y.H. Han, D.S. Kim, J.G. Mun, J. Park, M.Y. Jeong, S.H. Hong, Inhibitory effect of quercetin on colorectal lung metastasis through inducing apoptosis, and suppression of metastatic ability, *Phytomedicine* 23 (2016) 1680–1690. https://doi.org/10.1016/j.phymed.2016.09.011
10. A. Klimaszewska-Wiśniewska, M. Hałas-Wiśniewska, M. Izdebska, M. Gagat, A. Grzanka, D. Grzanka, Antiproliferative and antimetastatic action of quercetin on A549 non-small cell lung cancer cells through its effect on the cytoskeleton, *Acta Histochem.* 119 (2017) 99–112. https://doi.org/10.1016/j.acthis.2016.11.003
11. P. Wang, S.M. Henning, D. Heber, J.V. Vadgama, Sensitization to docetaxel in prostate cancer cells by green tea and quercetin, *J. Nutr. Biochem.* 26 (2015) 408–415. https://doi.org/10.1016/j.jnutbio.2014.11.017

12. H. Ji, Z. Zhang, C. Chen, W. Xu, T. Liu, Y. Dong, J. Wang, H. Wang, X. Zhu, The impact of quercetin and paclitaxel combination on ovarian cancer cells, *Iscience* 27 (2024) 110434. https://doi.org/10.1016/j.isci.2024.110434
13. L. Gibellini, M. Pinti, M. Nasi, S. De Biasi, E. Roat, L. Bertoncelli, A. Cossarizza, Interfering with ROS metabolism in cancer cells: the potential role of quercetin, *Cancers* 2 (2010) 1288–1311. https://doi.org/10.3390/cancers2021288
14. V. A. Kostyuk, A. I. Potapovich, Superoxide--driven oxidation of quercetin and a simple sensitive assay for determination of superoxide dismutase. *Biochemistry international* 19 (1989), 1117-1124.
15. D. Metodiewa, A. K. Jaiswal, N. Cenas, E. Dickancaité, J. Segura-Aguilar, Quercetin may act as a cytotoxic prooxidant after its metabolic activation to semiquinone and quinoidal product. *Free radical biology and medicine*, 26 (1999), 107-116. https://doi.org/10.1016/S0891-5849(98)00167-1
16. H.E. Hajji, E. Nkhili, V. Tomao, O. Dangles, Interactions of quercetin with iron and copper ions: complexation and autoxidation, *Free Radic. Res.* 40 (2006) 303–320. https://doi.org/10.1080/10715760500484351
17. M. Jiménez, F. García-Carmona, Oxidation of the flavonol quercetin by polyphenol oxidase, *J. Agric. Food Chem.* 47 (1999) 56–60. https://doi.org/10.1021/jf9805653
18. R. Baksi, D.P. Singh, S.P. Borse, R. Rana, V. Sharma, M. Nivsarkar, *In vitro* and *in vivo* anticancer efficacy potential of quercetin loaded polymeric nanoparticles, *Biomed. Pharmacother.* 106 (2018) 1513–1526. https://doi.org/10.1016/j.biopha.2018.07.106
19. A. Kumari, S.K. Yadav, Y.B. Pakade, B. Singh, S.C. Yadav, Development of biodegradable nanoparticles for delivery of quercetin, *Colloids Surf. B Biointerfaces* 80 (2010) 184–192. https://doi.org/10.1016/j.colsurfb.2010.06.002
20. A. Sarkar, S. Ghosh, S. Chowdhury, B. Pandey, P. C. Sil, Targeted delivery of quercetin loaded mesoporous silica nanoparticles to the breast cancer cells, *Biochim. Biophys. Acta Gen. Subj.* 1860 (2016) 2065–2075. https://doi.org/10.1016/j.bbagen.2016.07.001
21. P. Sadhukhan, M. Kundu, S. Chatterjee, N. Ghosh, P. Manna, J. Das, P.C. Sil, Targeted delivery of quercetin via pH-responsive zinc oxide nanoparticles for breast cancer therapy, *Mater. Sci. Eng. C* 100 (2019) 129–140. https://doi.org/10.1016/j.msec.2019.02.096
22. A. Sarkar, P.C. Sil, Iron oxide nanoparticles mediated cytotoxicity via PI3K/AKT pathway: role of quercetin, *Food Chem. Toxicol.* 71 (2014) 106–115. https://doi.org/10.1016/j.fct.2014.06.003
23. Y. Huang, J. Ren, X. Qu, Nanozymes: classification, catalytic mechanisms, activity regulation, and applications, *Chem. Rev.* 119 (2019) 4357–4412. https://doi.org/10.1021/acs.chemrev.8b00672
24. B. Jiang, D. Duan, L. Gao, M. Zhou, K. Fan, Y. Tang, X. Yan, Standardized assays for determining the catalytic activity and kinetics of peroxidase-like nanozymes, *Nat. Protoc.* 13 (2018) 1506–1520. https://doi.org/10.1038/s41596-018-0001-1
25. L. Gao, J. Zhuang, L. Nie, J. Zhang, Y. Zhang, N. Gu, X. Yan, Intrinsic peroxidase-like activity of ferromagnetic nanoparticles, *Nat. Nanotechnol.* 2 (2007) 577–583. https://doi.org/10.1038/nnano.2007.260
26. Z. Wang, X. Shen, X. Gao, Density functional theory mechanistic insight into the peroxidase- and oxidase-like activities of nanoceria, *J. Phys. Chem. C* 125 (2021) 23098–23104. https://doi.org/10.1021/acs.jpcc.1c04878
27. X. Zeng, H. Wang, Y. Ma, X. Xu, X. Lu, Y. Hu, J. Xie, X. Wang, Y. Wang, X. Guo, L. Zhao, J. Li, Vanadium oxide nanozymes with multiple enzyme-mimic activities for tumor catalytic therapy, *ACS Appl. Mater. & Interf.* 15 (2023), 13941-13955. https://doi.org/10.1021/acsami.2c20878
28. T. Chen, R. Huang, J. Liang, B. Zhou, X.L. Guo, X.C. Shen, B.P. Jiang, Natural polyphenol–vanadium oxide nanozymes for synergistic chemodynamic/photothermal therapy. *Chemistry–A European Journal*, 26 (2020), 15159-15169. https://doi.org/10.1002/chem.202002335
29. S. Li, Z. Chen, F. Yang, W. Yue, The age of vanadium-based nanozymes: Synthesis, catalytic mechanisms, regulation and biomedical applications. *Chinese Chemical Letters*, 35 (2024), p.108793. https://doi.org/10.1016/j.cclet.2023.108793
30. G. Grygorova, V. Seminko, N. Babayevska, M. Lupan, N. Kavok, S. Yefimova, Ultrasmall CeO_{2-x}@ß-CD nanoparticles with pH-dependent prooxidant activity and doxorubicin loading/release capability, *Phys. Chem. Chem. Phys.* 27 (2025) 23693–23705. https://doi.org/10.1039/D5CP02731D
31. B. Yang, Y. Chen, J. Shi, Reactive oxygen species (ROS)-based nanomedicine, *Chem. Rev.* 119 (2019) 4881–4985. https://doi.org/10.1021/acs.chemrev.8b00626
32. V. Seminko, and P. Maksimchuk, *Cerium Oxide Nanocrystals (CeO_{2-x}): Defects, Luminescence*

and Redox Activity. Springer Nature, 2026, 126 p. https://doi.org/10.1007/978-3-032-14130-9

33. P.O. Maksimchuk, K.O. Hubenko, V.V. Seminko, V.L. Karbivskii, A.S. Tkachenko, A.I. Onishchenko, S. L. Yefimova, High antioxidant activity of gadolinium–yttrium orthovanadate nanoparticles in cell-free and biological milieu. *Nanotechnology*, 33 (2022), 055701. https://doi.org/10.1088/1361-6528/ac31e5
34. M. Biler, D. Biedermann, K. Valentová, V. Křen, M. Kubala, Quercetin and its analogues: Optical and acido–basic properties, *Phys. Chem. Chem. Phys.* 19 (2017) 26870–26879. https://doi.org/10.1039/C7CP03845C
35. Y. Cai, W. Ren, C. Du, J. Zhang, Y. Zhao, J. Yu, T. Jiang, Cerium oxide nanozymes: exploring synthesis, catalytic activity, and biomedical potential, *Small* 21 (2025) 2504436. https://doi.org/10.1002/smll.202504436
36. A. Cornish-Bowden, One hundred years of Michaelis–Menten kinetics, *Perspect. Sci.* 4 (2015) 3–9. https://doi.org/10.1016/j.pisc.2014.12.002
37. X. Shen, Z. Wang, X.J. Gao, X. Gao, Reaction mechanisms and kinetics of nanozymes: insights from theory and computation, *Adv. Mater.* 36 (2024) 2211151. https://doi.org/10.1002/adma.202211151
38. Y. Yue, H. Wei, J. Guo, Y. Yang, Ceria-based peroxidase-mimicking nanozyme with enhanced activity: A coordination chemistry strategy, *Colloids Surf. A Physicochem. Eng. Asp.* 610 (2021) 125715. https://doi.org/10.1016/j.colsurfa.2020.125715
39. Y. Wu, L. Yang, Q. Wu, Q. Liu, L. Zou, X. Yang, K. Tang, Regulation of the oxidase mimetic activity of ceria nanoparticles by buffer composition, *Chem. Eur. J.* 29 (2023) e202204071. https://doi.org/10.1002/chem.202204071
40. K. Reed, A. Cormack, A. Kulkarni, M. Mayton, D. Sayle, F. Klaessig, B. Stadler, Exploring the properties and applications of nanoceria: is there still plenty of room at the bottom?, *Environ. Sci. Nano* 1 (2014) 390–405. https://doi.org/10.1039/C4EN00079J
41. I. Celardo, J.Z. Pedersen, E. Traversa, L. Ghibelli, Pharmacological potential of cerium oxide nanoparticles, *Nanoscale* 3 (2011) 1411–1420. https://doi.org/10.1039/C0NR00875C
42. V. Seminko, P. Maksimchuk, G. Grygorova, E. Okrushko, O. Avrunin, V. Semenets, Y. Malyukin, Mechanism and dynamics of fast redox cycling in cerium oxide nanoparticles at high oxidant concentration, *J. Phys. Chem. C* 125 (2021) 4743–4749. https://doi.org/10.1021/acs.jpcc.1c00382
43. P.O. Maksimchuk, K.O. Hubenko, V.V. Seminko, V.L. Karbivskii, A.S. Tkachenko, A.I. Onishchenko, S.L. Yefimova, High antioxidant activity of gadolinium–yttrium orthovanadate nanoparticles in cell-free and biological milieu, *Nanotechnology* 33 (2022) 055701. https://doi.org/10.1088/1361-6528/ac31e5